

Two mass conjectures on axially symmetric black hole–disk systems.

Wojciech Kulczycki, Patryk Mach, and Edward Malec

Instytut Fizyki im. Mariana Smoluchowskiego, Uniwersytet Jagielloński, Łojasiewicza 11, 30-348 Kraków, Poland

We analyze stationary self-gravitating disks around spinning black holes that satisfy the recently found general-relativistic Keplerian rotation law. There is a numerical evidence that the angular velocity, circumferential radius and angular momenta yield a bound onto the asymptotic mass of the system. This bound is proven analytically in the special case of massless disks of dust in the Kerr spacetime.

PACS numbers: 04.20.-q, 04.25.Nx, 04.40.Nr, 95.30.Sf

I. INTRODUCTION

Angular velocities Ω of test bodies in a nonrelativistic Keplerian circular motion encode information about central masses. The central mass is inferred to be $\Omega^2 r_C^3/G$, where G is the gravitational coupling constant and r_C denotes the circumferential radius of the orbit of the body. Recent numerical analysis suggests that one can estimate the total mass m also for a system with selfgravitating fluids in Keplerian rotation around a spherical centre, $\Omega^2 r_C^3/G \leq m$ [1, 2]. In this paper we shall investigate general-relativistic selfgravitating disks or toroids around spinning central black holes. We shall propose two modified inequalities for selfgravitating rotating systems in the general-relativistic Keplerian motion [3, 4]; they imply $\Omega r_C^{3/2} \leq \sqrt{GM_{\text{ADM}}} + \frac{2|a|}{\sqrt{r_C}}$, where a and M_{ADM} are the spin parameter of the black hole and the asymptotic mass of the whole configuration, respectively. There is a rich numerical evidence, some reported in what follows, that supports our conjecture.

The question of estimating masses or determining rotation curves in toroidal systems has been addressed, within Newtonian physics, in the astrophysical literature [5–9]. We would like to stress that our methods are different and we work within the general relativistic context.

For simplicity, we assume only polytropic fluids rotating around a (spinning or spinless) black hole, but we take into account the selfgravity of the fluid. Stationary axially symmetric systems of rotating barotropic fluids need the so-called rotation curve, that tells particles of fluid how to rotate. They are described by the free-boundary elliptic systems of partial differential equations—the shape of rotating fluids cannot be set *a priori*, but comes with the solution. There exists a numerical technology to deal with such problems, developed by many authors (a sample of sources: [10–14]), but the number of analytical results on the existence of solutions is small. There is a paper concerning self-gravitating fluids in Newtonian gravity [15] and a research on rigid rotations of self-gravitating gases in general relativity [16–18].

In Newtonian gravity the Poincaré-Wavre theorem restricts allowed rotations curves to $\Omega = \Omega(r_C)$, where the circumferential radius r_C is equal to the distance from the rotation axis. They obviously include the Keplerian rotation law. The general-relativistic rotation

has been investigated since early 1970's — primarily a rigid rotation [19, 20] and its modifications [21–23]. New general-relativistic differential rotation laws $j = j(\Omega)$, where j denotes the specific angular momentum, have recently been found for stationary systems consisting of self-gravitating toroids around spinless [24, 25] and spinning black holes [3, 4]. They describe, in particular, the motion of a massless disks of dust, with $\Omega = \sqrt{GM_{\text{ADM}}}/r_C^{3/2}$ in the case of the Schwarzschild geometry. In the nonrelativistic limit one has the monomial rotation law $\Omega = w/r_C^\lambda$ ($0 \leq \lambda \leq 2$); that obviously includes the Keplerian rotation law.

The order of the main part of this paper is as follows. Section II describes formalism. Section III contains two main conjectures concerning masses of axially symmetric stationary systems with black holes. In Section IV we show that test-like disks of dust satisfy the two mass conjectures in Schwarzschild and Kerr geometries. The proof concerning the Kerr spacetime is relegated to the Appendix. Section V presents a sample of numerical examples that confirm our two conjectures.

II. EQUATIONS

We assume a *stationary* metric of the form

$$ds^2 = -\alpha^2 dt^2 + r^2 \sin^2 \theta \psi^4 (d\varphi + \beta dt)^2 + \psi^4 e^{2q} (dr^2 + r^2 d\theta^2). \quad (1)$$

Here t is the time coordinate, and r, θ, φ are spherical coordinates. In the general-relativistic part of this paper the gravitational constant $G = 1$ and the speed of light $c = 1$. We assume axial symmetry and employ the stress-momentum tensor

$$T^{\alpha\beta} = \rho h u^\alpha u^\beta + p g^{\alpha\beta},$$

where ρ is the baryonic rest-mass density, h is the specific enthalpy, and p is the pressure. Metric functions α, ψ, q and β in (1) depend on r and θ only.

The following method can be applied to any barotropic equation of state, but we will deal with polytropes $p(\rho) = K\rho^\gamma$. Then one has the specific enthalpy

$$h(\rho) = 1 + \frac{\gamma p}{(\gamma - 1)\rho}.$$

The 4-velocity $(u^\alpha) = (u^t, 0, 0, u^\varphi)$ is normalized, $g_{\alpha\beta}u^\alpha u^\beta = -1$. The coordinate angular velocity reads

$$\Omega = \frac{u^\varphi}{u^t}. \quad (2)$$

We define the angular momentum per unit inertial mass ρh [26]

$$j \equiv u_\varphi u^t. \quad (3)$$

It is known since early 1970's that general-relativistic Euler equations are solvable under the condition that $j \equiv j(\Omega)$ [19, 20]. Within the fluid region, the Euler equations $\nabla_\mu T^{\mu\nu} = 0$ can be integrated,

$$\int j(\Omega) d\Omega + \ln\left(\frac{h}{u^t}\right) = C. \quad (4)$$

In [24] we have had the rotation law

$$j(\Omega) \equiv \frac{\tilde{w}^{1-\delta}\Omega^\delta}{1 - \kappa\tilde{w}^{1-\delta}\Omega^{1+\delta} + \Psi}; \quad (5)$$

here Ψ is of the order of the binding energy per unit baryonic mass and w , δ , and $\kappa = (1 - 3\delta)/(1 + \delta)$ are parameters. This law was obtained in a procedure involving an ‘‘educated guess-work’’ [24].

Equation (5) can be transformed (through a rescaling of \tilde{w}) into

$$j(\Omega) \equiv \frac{w^{1-\delta}\Omega^\delta}{1 - \kappa w^{1-\delta}\Omega^{1+\delta}} = (-\kappa\Omega + w^{\delta-1}\Omega^{-\delta})^{-1},$$

The Keplerian rotation corresponds to the parameter $\delta = -1/3$ and $\kappa = 3$; it is interpreted as a rotation law for the fluid around a spin-less black hole.

The rotation law describing motion of gaseous tori around spinning black holes,

$$j(\Omega) = -\frac{1}{2} \frac{d}{d\Omega} \ln \left\{ 1 - \left[\tilde{a}^2 \Omega^2 + 3w^{\frac{4}{3}} \Omega^{\frac{2}{3}} (1 - \tilde{a}\Omega)^{\frac{4}{3}} \right] \right\}, \quad (6)$$

has been found in [3, 4]. Here \tilde{a} is a kind of a bare spin parameter of a black hole (see a comment below); it coincides with the Kerr spin parameter for massless disks of dust.

The rotation curves—angular velocities as functions of spatial coordinates $\Omega(r, \theta)$ —can be recovered from Eq. (3),

$$j(\Omega) = \frac{V^2}{(\Omega + \beta)(1 - V^2)}. \quad (7)$$

Here the squared linear velocity is given by

$$V^2 = r^2 \sin^2 \theta (\Omega + \beta)^2 \frac{\psi^4}{\alpha^2}.$$

Following [13] we introduce the central black hole using the puncture method [27]. The black hole is surrounded

by a minimal two-surface S_{BH} (the horizon) embedded in a fixed hypersurface of constant time, and located at $r = r_s = \sqrt{m^2 - \tilde{a}^2}/2$, where m is a mass parameter. Its area defines the irreducible mass $M_{\text{irr}} = \sqrt{\frac{A_{\text{BH}}}{16\pi}}$ and its angular momentum J_{BH} follows from the Komar expression

$$J_{\text{BH}} = \frac{1}{4} \int_0^{\pi/2} \frac{r^4 \psi^6}{\alpha} \partial_r \beta \sin^3 \theta d\theta. \quad (8)$$

In this construction the angular momentum is given rigidly on the event horizon S_{BH} , in terms of data taken from the Kerr solution and independently of the content of mass in a torus, $J_{\text{BH}} = m\tilde{a}$ [13]. The mass of the black hole is then defined in terms of the irreducible mass and the angular momentum,

$$M_{\text{BH}} = M_{\text{irr}} \sqrt{1 + \frac{J_{\text{BH}}^2}{4M_{\text{irr}}^4}}. \quad (9)$$

We define the black hole spin parameter as $a = J_{\text{BH}}/M_{\text{BH}}$. If the disk is sufficiently massive (self-gravitating), we have in general $a \neq \tilde{a}$ [3, 4]. If the self-gravity of the torus can be neglected, then $M_{\text{BH}} = m$, $a = \tilde{a}$, and the metric of the spacetime coincides (by construction) with the Kerr solution.

Asymptotic (total) mass M_{ADM} and angular momentum J_{ADM} can be defined as appropriate Arnowitt-Deser-Misner charges, and they can be computed by means of corresponding volume integrals [13].

A circumferential radius corresponding to the circle $r = \text{const}$ on the symmetry plane $\theta = \pi/2$ is given by

$$r_C = r\psi^2. \quad (10)$$

The numerical part of this paper is based on the scheme described in [3, 4]. In the rest of the paper we always assume that $\Omega > 0$. Corotating disks have $a > 0$, while counterrotating disks have negative spins: $a < 0$.

III. TWO MASS CONJECTURES

General-relativistic Keplerian systems with tori are characterized by their asymptotic masses M_{ADM} and angular momenta J_{ADM} , and the quasilocal characteristics of central black holes—the mass M_{BH} and the angular momentum J_{BH} . It is clear that in the Newtonian limit we should get $\Omega r_C^{3/2} \leq \sqrt{m}$ [1, 2]. From this, and from the dimensional analysis, one may guess that $\Omega r_C^{3/2} \leq \sqrt{M_{\text{ADM}}} + 2 \frac{|J_X|}{m_Y \sqrt{r_C}}$, where $X, Y = \text{BH, ADM}$. The asymptotic mass is larger than the mass of the central black hole, but the angular momentum is not monotonic — the asymptotic angular momentum might be smaller than J_{BH} . That means that there are two independent possibilities.

Conjecture 1.

$$\Omega r_C^{3/2} \leq \sqrt{M_{\text{ADM}}} + \frac{2|J_{\text{ADM}}|}{M_{\text{ADM}}\sqrt{r_C}}. \quad (11)$$

Conjecture 2.

$$\Omega r_C^{3/2} \leq \sqrt{M_{\text{ADM}}} + \frac{2|J_{\text{BH}}|}{M_{\text{ADM}}\sqrt{r_C}}. \quad (12)$$

Notice that $\frac{|J_{\text{BH}}|}{M_{\text{ADM}}} \leq |a|$, where a is the black hole spin parameter. Thus Conjecture 2 implies $\Omega r_C^{3/2} \leq \sqrt{M_{\text{ADM}}} + \frac{2|a|}{\sqrt{r_C}}$.

Numerical calculations reported in Sec. VI suggest the validity of both Conjectures. They coincide for test disks of dust in the Kerr geometry, since then $M_{\text{BH}} = M_{\text{ADM}}$ and $J_{\text{ADM}} = J_{\text{BH}}$. The inequality reduces to the equality in the Schwarzschild spacetime and it is satisfied in Kerr spacetimes (see the Appendix for an algebraic proof).

The inspection of both inequalities (11) and (12) shows that far from the center the corresponding expressions on the right-hand sides are expected to be constant; if a toroid is light and large, then $\Omega r_C^{3/2}$ is expected to be close to $\sqrt{M_{\text{ADM}}}$ (see Sec. V). The inspection of these inequalities in the interior might give some information about angular momentum.

IV. ANGULAR MOMENTUM AND MASS ESTIMATES IN KERR AND SCHWARZSCHILD SPACETIMES

A. Kerr geometry in conformal coordinates

Define

$$r_K = r \left(1 + \frac{m}{r} + \frac{m^2 - a^2}{4r^2} \right), \quad (13)$$

$$\Delta_K = r_K^2 - 2r_K + a^2,$$

and

$$\Sigma_K = r_K^2 + a^2 \cos^2 \theta.$$

The Kerr metric can be written in form (1) as follows [13, 27]. The conformal factor ψ_K reads

$$\psi_K = \frac{1}{\sqrt{r}} \left(r_K^2 + a^2 + 2ma^2 \frac{r_K \sin^2 \theta}{\Sigma_K} \right)^{1/4}. \quad (14)$$

The only component β_K of the shift vector is given by

$$\beta_K = -\frac{2mar_K}{(r_K^2 + a^2)\Sigma_K + 2ma^2 r_K \sin^2 \theta}. \quad (15)$$

Finally, the functions α_K and q_K are defined as

$$\alpha_K = \left(\frac{\Sigma_K \Delta_K}{(r_K^2 + a^2)\Sigma_K + 2ma^2 r_K} \sin^2 \theta \right)^{1/2},$$

$$e^{q_K} = \frac{\Sigma_K}{\sqrt{(r_K^2 + a^2)\Sigma_K + 2ma^2 r_K \sin^2 \theta}}. \quad (16)$$

The surface $r = r_s \equiv \frac{1}{2}\sqrt{m^2 - a^2}$ is an apparent horizon, that coincides with the event horizon.

Test particles can rotate along circular orbits $r = \text{const}$ in the Kerr geometry. That implies the existence of a test-like disk made of dust, that moves circularly and lies in the plane $\theta = \pi/2$. Its angular velocity reads

$$\Omega(r) = \frac{8r^{3/2}}{((2r+1)^2 - a^2)^{3/2} + 8ar^{3/2}}. \quad (17)$$

The dragging angular velocity of the Kerr space-time is given by $\Omega_d = -\beta_K$, that is

$$\Omega_d = \frac{2ma}{r_K(r_K^2 + a^2) + 2ma^2}. \quad (18)$$

The circumferential radius of this circular orbit is equal to

$$r_C = r\psi^2 = \sqrt{r_K^2 + a^2 + \frac{2ma^2}{r_K}} \quad (19)$$

It is clear that

$$\Omega_d = \frac{2ma}{r_K r_C^2}. \quad (20)$$

It appears that the product $\Omega r_C^{3/2}$ exceeds the value \sqrt{m} for all strictly negative spin parameters a and for $a > 0.9525$. There exists, however, a modified inequality that takes into account the dragging effects and that is always true:

$$\Omega r_C^{3/2} \leq \sqrt{m} + |\Omega_d| r_C^{3/2} = \sqrt{m} + \frac{2m|a|}{r_K r_C^{1/2}}. \quad (21)$$

The proof of (21) is relegated to the Appendix.

The quantity $m|a|$ is the absolute value $|J_{\text{BH}}|$ of the angular momentum, while $r_K \geq m$ outside the region encircled by the trapped surface $r = r_s$. Thus for a disk in Keplerian motion around a Kerr black hole we have

$$\Omega r_C^{3/2} \leq \sqrt{m} + 2 \frac{J_{\text{BH}}}{m\sqrt{r_C}} = \sqrt{m} + 2 \frac{|a|}{\sqrt{r_C}}. \quad (22)$$

This agrees with both inequalities (11) and (12), since they coincide in this case.

B. Schwarzschild geometry

Schwarzschild space-time in conformal coordinates is given by metric functions of the preceding subsection assuming the spin parameter $a = 0$. Test bodies in a Schwarzschild space-time can move on circular orbits with the angular velocity $\Omega = \frac{\sqrt{m}}{r_C^{3/2}}$. Thus there exist massless disks, consisting of particles of dust, with the rotation law $\Omega = \frac{\sqrt{m}}{r_C^{3/2}}$. This implies the strict equality $\Omega r_C^{3/2} = \sqrt{m}$; the inequalities (11) and (12) coincide, and they are saturated.

V. NUMERICAL RESULTS

In this section we deal with numerical solutions describing self-gravitating fluids around black holes. The numerical method was described in detail in [3, 4].

It is convenient to rewrite inequalities (11) and (12) in the following form.

i) Conjecture 1.

$$\max\left((\Omega - \Omega_{d,1})r_C^{3/2}\right) \leq \sqrt{M_{\text{ADM}}}; \quad (23)$$

$$\text{here } \Omega_{d,1} = \frac{2|J_{\text{ADM}}|}{M_{\text{ADM}}r_C^2}.$$

ii) Conjecture 2.

$$\max\left((\Omega - \Omega_{d,2})r_C^{3/2}\right) \leq \sqrt{M_{\text{ADM}}}; \quad (24)$$

$$\text{here } \Omega_{d,2} = \frac{2|J_{\text{BH}}|}{M_{\text{ADM}}r_C^2}.$$

We performed a large number of numerical calculations, with equations of state $p = K\rho^{4/3}$ and $p = K\rho^{5/3}$, for a range of values of the spin parameter a , the radius of the inner boundary r_1 and for several values of the maximal mass density ρ_{max} . In this paper we report only results concerning the polytrope with the polytropic index $\gamma = 4/3$, but the other case gives similar results. In numerical solutions of Figs. 1 and 2 we fix the coordinate radius of the disk's outer boundary $r_2 = 20$, but the inner radius r_1 is changed, within limits shown in captions of Figures. Figures 3–5 are dedicated to the analysis of $\Omega r_C^{3/2}$ in specific solutions. In all cases we calculated values of the left hand sides of (23) and (24) in the symmetry plane $\theta = \pi/2$.

Figure 1 summarizes results of more than four hundred (counter-rotating) numerical solutions. The diagram shows maximal values of the left hand sides of (23) and (24) in units of the square root of the asymptotic mass. There is a sharp spike in the diagram corresponding to Conjecture 1 (see (23)); around $r_1 = 11.7$ the angular momentum of the disk cancels the black hole spin. The asymptotic angular momentum J_{ADM} decreases, vanishes at the top of the spike and becomes

more and more negative. Conjecture 2 is also satisfied, but the expression $\max((\Omega - \Omega_{d,2})r_C^{3/2})/\sqrt{M_{\text{ADM}}}$ changes only moderately. Figure 2 presents results of more than seven hundred (co-rotating) numerical solutions. It is clear that both proposed conjectures, 1 and 2, are valid in our numerical calculations, for co- and counter-rotating systems.

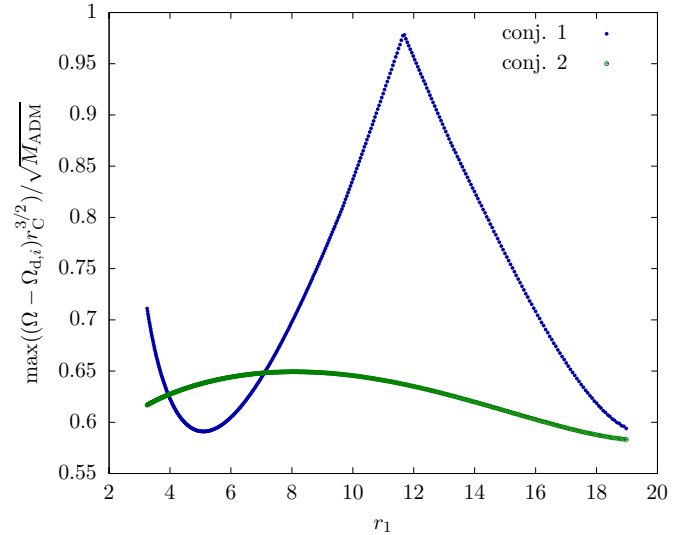


FIG. 1. Maximal values of left hand-sides of Conjectures 1 (conj. 1) and 2 (conj. 2) for $\gamma = 4/3$, $\tilde{a} = -0.99$ and $\rho_{\text{max}} = 3.0 \times 10^{-4}$. Here $r_2 = 20$ and r_1 varies from 6.01 to 18.97. Asymptotic masses are in the range (1.005, 1.46). Each point on the diagram corresponds to a solution.

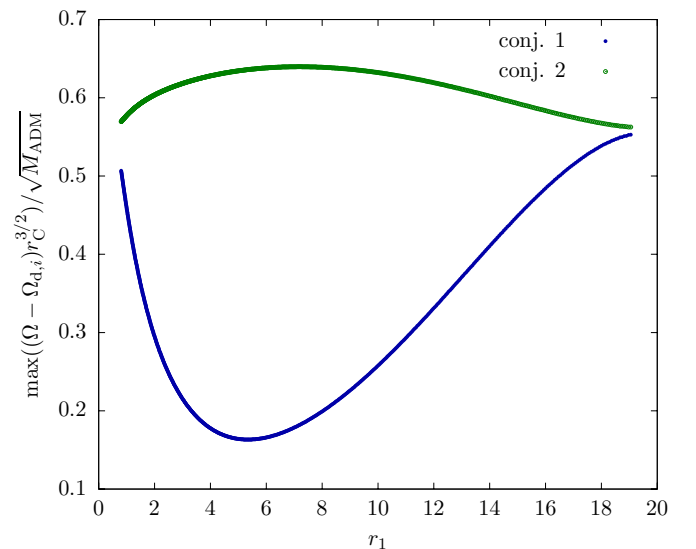


FIG. 2. Maximal values of left hand-sides of Conjectures 1 and 2 for $\gamma = 4/3$, $\tilde{a} = 0.99$ and $\rho_{\text{max}} = 3.0 \times 10^{-4}$. Here $r_2 = 20$ and r_1 varies from 0.805 to 19.05. Asymptotic masses are in the range (1.005, 1.46). Each point on the diagram corresponds to a solution.

Figure 3 shows the behaviour of the product $\Omega r_C^{3/2}$ on

the symmetry plane of a compact disk—its outer circumferential radius is less than 21.6 and the asymptotic mass $M_{\text{ADM}} \in (1.45, 1.47)$ while the mass of the central black hole is $M_{\text{BH}} = 1.02$. We display two curves, for $a = 0.49$ and $a = -0.485$. The dependence on the spin is more pronounced in disk's interior and becomes negligible in disk's peripherals.

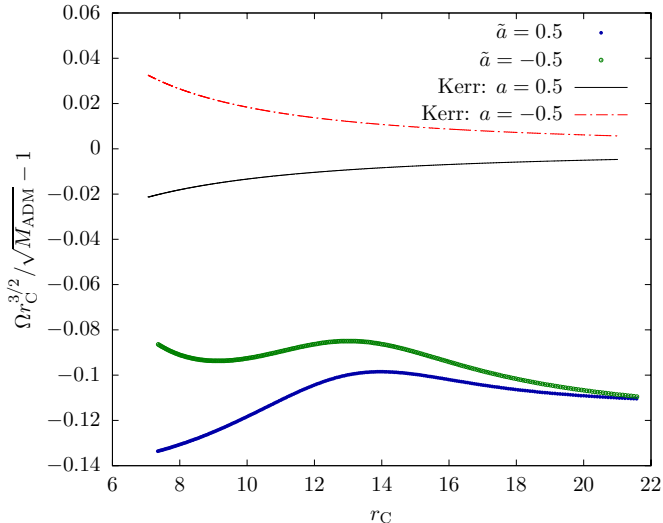


FIG. 3. The plot of $\frac{\Omega r_C^{3/2}}{\sqrt{M_{\text{ADM}}}} - 1$ as function of r_C . Here $\gamma = 4/3$ and $\rho_{\text{max}} = 3.0 \times 10^{-4}$. i) Blue line: $a = 0.49$, $r_C \in (7.35, 21.57)$, $M_{\text{ADM}} = 1.45$ and $M_{\text{BH}} = 1.02$. ii) Green line: $a = -0.485$, $r_C \in (7.36, 21.58)$, $M_{\text{ADM}} = 1.47$ $M_{\text{BH}} = 1.03$. iii) For the comparison, the plot of $\frac{\Omega r_C^{3/2}}{m} - 1$ for a massless disk in the Kerr geometry, with $m = 1$.

Figure 4 shows the behaviour of the product $\Omega r_C^{3/2}$ on the symmetry plane of the disk. The disk is quite extended and somewhat heavier—its outer circumferential radius is larger than 100 and the asymptotic mass $M_{\text{ADM}} = 2$ while the mass of the black hole is $M_{\text{BH}} = 1.02$. We display two curves, for $a = 0.49$ and $a = -0.49$. The dependence on the spin is seen in disk's interior and becomes negligible in disk's peripherals.

Figure 5 shows the same as Fig. 4, but the spin is higher. Again the disk is extended but it is light—its outer circumferential radius is larger than 100 and the asymptotic mass $M_{\text{ADM}} = 1.1$ while the mass of the black hole is $M_{\text{BH}} = 1.00$. We display two curves, for $a = 0.99$ and $a = -0.99$. A strong dependence on the spin is seen in disk's interior, but it is noticeable even in disk's peripherals. Notice that $\sup(\Omega r_C^{3/2}) > 1.1$ for the two counter-rotating branches, but only the massless co-rotating branch has $\Omega r_C^{3/2}$ exceeding 1.

It is instructive to compare the two self-gravitating solutions in Fig. 3 with the two massless disks of dust in the Kerr geometry. It is clear that the self-gravity merely pushes down the value of $\Omega r_C^{3/2}/M_{\text{ADM}} - 1$ obtained for dust solutions in Kerr space-times. The branch corresponding to the counter-rotation remains above the

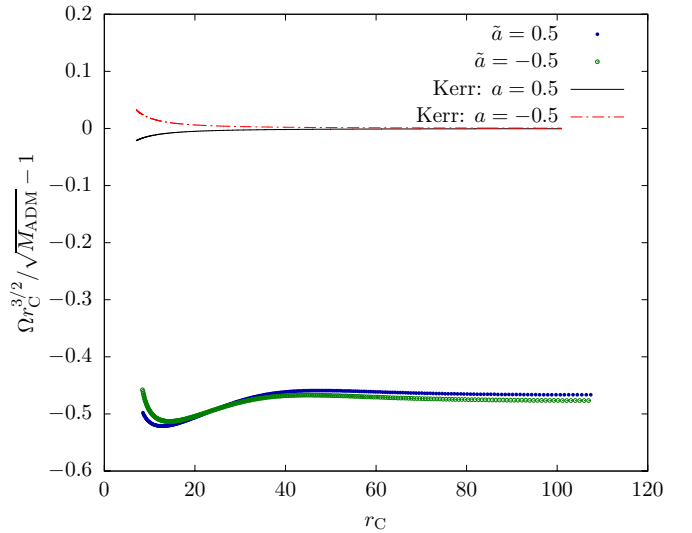


FIG. 4. The plot of $\frac{\Omega r_C^{3/2}}{\sqrt{M_{\text{ADM}}}} - 1$ as function of r_C . Here $\gamma = 4/3$, $r_C \in (7.27, 102.32)$, $M_{\text{ADM}} = 2$ and $M_{\text{BH}} = 1.02$. i) Blue line: $a = 0.49$, $\rho_{\text{max}} = 7.47 \times 10^{-6}$. ii) Green line: $a = -0.49$, $\rho_{\text{max}} = 7.74 \times 10^{-6}$. iii) For the comparison, the plot of $\frac{\Omega r_C^{3/2}}{m} - 1$ for a massless disk in the Kerr geometry, with $m = 1$.

co-rotating one, but they almost coincide at the outer boundary. A similar picture is seen in Fig. 5. We see the same effect in Fig. 4, but with a more pronounced shift downwards. The co-rotating and counter-rotating branches cross around $r_C \approx 30$ and then their positions do reverse. Thus the more massive is the rotating toroid, the stronger the self-gravity impacts the quantity $\Omega r_C^{3/2}$. Figure 5 demonstrates yet another influence of the self-gravity; the inner boundary of the co-rotating toroid shifts upwards from $r_C = 2.108$ (in the Kerr spacetime) to $r_C = 2.32$ and of the counter-rotating toroid moves downwards from $r_C = 9.04$ (in the Kerr spacetime) to $r_C = 4.68$.

VI. SUMMARY

The two conjectures on masses of rotating systems are based partly on analytic arguments and partly on extensive numerical data. Their proof would pose a serious analytic challenge.

We envisage two further applications. The first concerns astrophysics. Rotating axially symmetric systems are quite common. They are known to exist in some active galactic nuclei. Particularly interesting are those containing supermasers. Our inequalities might be useful in extracting information about masses and angular momenta, provided that more information on modelling of AGN's with toroids becomes available.

The two statements of (11) and (12) can be useful in estimating the amount of angular momentum within a fixed volume. There is already a formidable work done in

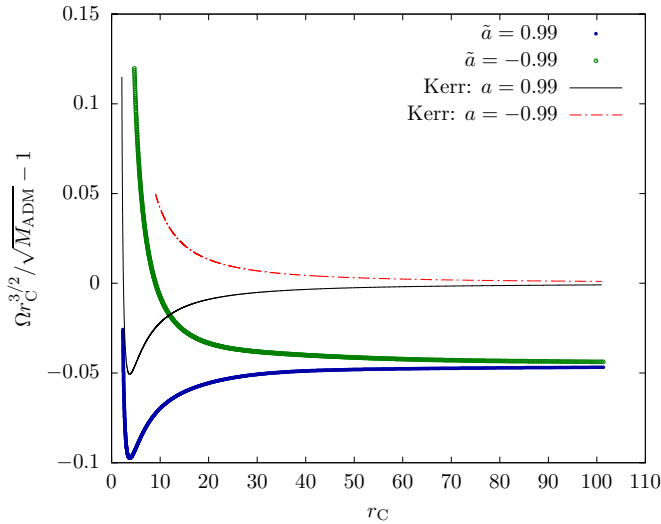


FIG. 5. The plot of $\frac{\Omega r_C^{3/2}}{M_{ADM}} - 1$ as function of r_C . Here $\gamma = 4/3$, $M_{ADM} = 1.1$ and $M_{BH} = 1.00$. i) Green line: $a = -0.99$, $\rho_{max} = 1.92 \times 10^{-6}$, $r_C \in (4.68, 101.36)$. ii) Blue line: $a = 0.99$, $\rho_{max} = 2.5 \times 10^{-6}$, $r_C \in (2.32, 101.36)$. iii) For the comparison, the plot of $\frac{\Omega r_C^{3/2}}{m} - 1$ for a massless disk in the Kerr geometry ($m = 1$). For $a = -0.99$: $r_C \in (9.04, 101.00)$, while for $a = 0.99$: $r_C \in (2.108, 101.00)$.

this direction [29, 30], although results are far from being precise [14]. We think that (11) and (12) are true and they would lead to substantial improvements of present estimates.

VII. APPENDIX. PROOF OF THE MASS INEQUALITY IN THE KERR GEOMETRY

We shall do this proof in Boyer-Lindquist coordinates (r_K, θ, ϕ) , where the Boyer-Lindquist radius r_K relates to the conformal radius r via formula (13) [27]. The metric takes on the standard form

$$\begin{aligned}
 ds^2 = & - \left(1 - \frac{2mr_K}{\Sigma_K} \right) dt^2 + \frac{\Sigma_K}{\Delta_K} dr_K^2 + \\
 & \Sigma_K d\theta^2 + \frac{\Delta_K \Sigma_K + 2mr_K(r_K^2 + a^2)}{\Sigma_K} \sin^2 \theta d\phi^2 - \\
 & \frac{4mr_K a \sin^2 \theta}{\Sigma_K} dt d\phi,
 \end{aligned} \tag{25}$$

where $\Sigma_K = r_K^2 + a^2 \cos^2 \theta$, $\Delta_K = r_K^2 - 2mr_K + a^2$.

The inequalities of Section V are expressed in terms of geometric quantities, hence they are independent of the choice of coordinates within a fixed Cauchy slice. We shall consider a massless disk, that is located in the symmetry plane $\theta = \pi/2$.

A. Geometric quantities

The angular velocity Ω reads

$$\Omega = \frac{u^\phi}{u^t} = \frac{\sqrt{m}}{r_K^{3/2} + a\sqrt{m}}. \tag{26}$$

The circular radius r_C can be expressed as follows, in the symmetry plane:

$$r_C = \sqrt{r_K^2 + a^2 + \frac{2ma^2}{r_K}}. \tag{27}$$

The angular velocity due to dragging plays a significant role in the calculation. It is given by

$$\Omega_d = \frac{2ma}{r_C^2 r_K}. \tag{28}$$

The irreducible mass of the Kerr black hole reads

$$M_{irr} = \frac{m}{2} \sqrt{2 \left(1 + \sqrt{1 - \frac{a^2}{m^2}} \right)}. \tag{29}$$

The quantity r_{ISCO} denotes the coordinate radius of the innermost stable circular orbit (ISCO), that depends on a and m . In the case of co-rotation $r_{ISCO} \geq m$ (with the equality when $a = 1$) while in the case of counter-rotation $6m \leq r_{ISCO} \leq 9m$ (with the upper bound saturated for $a = -1$).

B. Proofs

We shall prove analytically the validity of the following inequality, provided that the areal radius is not smaller than r_{ISCO} : $r_K \geq r_{ISCO}$:

$$\Omega r_C^{3/2} \leq \sqrt{m} + |\Omega_d| r_C^{3/2}. \tag{30}$$

For the simplicity, but without the loss of generality, we shall put $m = 1$.

We divide both sides of (30) by $r_C^{3/2}$; that leads to

$$\Omega - |\Omega_d| \leq \sqrt{\frac{1}{r_C^3}}. \tag{31}$$

Using (13, 26–29), one arrives at

$$\begin{aligned}
 & \frac{1}{r_K^{3/2} + a} - \frac{2|a|}{r_K(r_K^2 + a^2) + 2a^2} \leq \\
 & \leq \left(a^2 + \frac{2a^2}{r_K} + r_K^2 \right)^{-3/4}.
 \end{aligned} \tag{32}$$

a. The case $a = 0$ corresponds to the Schwarzschild geometry and it has been already discussed.

b. In the corotating case, $a > 0$, inequality (32) takes the form

$$\frac{1}{r_K^{3/2} + a} - \frac{2a}{r_K(r_K^2 + a^2) + 2a^2} \leq \left(a^2 + \frac{2a^2}{r_K} + r_K^2\right)^{-3/4}. \quad (33)$$

It is easy to show that the left hand side of this inequality is non-negative, since (as we show below) for $r_K \geq r_{\text{ISCO}}$,

$$r_K(r_K^2 - 2a\sqrt{r_K} + a^2) \geq 0. \quad (34)$$

Indeed, notice that $r_K \geq \sqrt{r_K}$; this is so because $r_{\text{ISCO}} \geq 1$. But that implies $(r_K^2 - 2a\sqrt{r_K} + a^2) \geq (r_K - a)^2$, which is obviously non-negative. That in turn implies the non-negativity of (34). Therefore the sign of the inequality (33) does not reverse when we calculate the quartic power of both sides,

$$0 \leq \frac{r_K^3}{(r_K(r_K^2 + a^2) + 2a^2)^4 (r_K^{3/2} + a)^4} \times \left[(r_K(r_K^2 + a^2) + 2a^2)(r_K^{3/2} + a)^4 - r_K(r_K^2 - 2ar_K^{1/2} + a^2)^4 \right]. \quad (35)$$

The denominator of (35) is positive for $r_K \geq r_{\text{ISCO}} \geq 1$. One can find out, using the REDUCE function of Mathematica [28], that the numerator of (35) is also non-negative, if r_K is not smaller than 1.

c. The counter-rotating case $a < 0$. Changing $a \rightarrow -|a|$ in the inequality (32), one arrives at

$$\frac{1}{r_K^{3/2} - |a|} - \frac{2|a|}{r_K(r_K^2 + a^2) + 2a^2} \leq \left(a^2 + \frac{2a^2}{r_K} + r_K^2\right)^{-3/4}. \quad (36)$$

It is easy to show that the left hand side of this inequality is nonpositive, if and only if

$$r_K^3 - 2ar_K^{3/2} + a^2(4 + r_K) \geq 0. \quad (37)$$

However for $r_K \geq 0$:

$$\begin{aligned} & r_K^3 - 2|a|r_K^{3/2} + a^2(4 + r_K) \geq \\ & \geq r_K^3 - 2|a|r_K^{3/2} + 4a^2 = (r_K^{3/2} - |a|)^2 + 3a^2, \end{aligned}$$

which is manifestly non-negative. Thus the left-hand side of (36) is non-negative for $r \geq r_K$. Again we can calculate the quartic power of both sides,

$$0 \leq \frac{1}{(r_K(r_K^2 + |a|^2) + 2|a|^2)^4 (r_K^{3/2} - |a|)^4} \times \left[r_K^3(r_K(r_K^2 + |a|^2) + 2|a|^2)(r_K^{3/2} - |a|)^4 - (r_K^3 - 2|a|r_K^{3/2} + |a|^2(4 + r_K))^4 \right]. \quad (38)$$

The denominator of (38) is positive for $r_K \geq 1$. One can find out, using the REDUCE function of Mathematica [28], that the numerator is also non-negative, if r_K is not smaller than 6. In conclusion, in the interval of interest for counter-rotation ($r_K > r_{\text{ISCO}} \geq 6$) inequality (36) holds true.

ACKNOWLEDGMENTS

This research was carried out with the supercomputer “Deszno” purchased thanks to the financial support of the European Regional Development Fund in the framework of the Polish Innovation Economy Operational Program (Contract no. POIG. 02.01.00-12-023/08).

-
- [1] P. Mach, E. Malec, and M. Piróg, Estimating masses of Keplerian disk systems: the case of AGN in NGC 4258, *Acta Phys. Pol. B* **43**, 2141 (2012).
 - [2] P. Mach, E. Malec, and M. Piróg, Geometry of Keplerian disk systems and bounds on masses of their components, *Acta Phys. Pol. B* **44**, 107 (2013).
 - [3] J. Karkowski, W. Kulczycki, P. Mach, E. Malec, A. Odrzywołek, and M. Piróg, General-relativistic rotation: Self-gravitating fluid tori in motion around black holes, *Phys. Rev. D* **97**, 104034 (2018).
 - [4] J. Karkowski, W. Kulczycki, P. Mach, E. Malec, A. Odrzywołek, and M. Piróg, Self-gravitating axially symmetric disks in general-relativistic rotation, *Phys. Rev. D* **97**, 104017 (2018).
 - [5] J.-M. Huré, Origin of the non-Keplerian motion of masers in NGC 1068, *Astron. Astrophysics* **395**, L21 (2002).
 - [6] L. J. Greenhill, C. R. Gwinn, R. Antonucci, and R. Barvainis, VLBI Imaging of Water Maser Emission from the Nuclear Torus of NGC 1068, *Astrophys. J.* **472**, L21 (1996).
 - [7] G. Lodato and G. Bertin, Non-Keplerian rotation in the nucleus of NGC 1068: Evidence for a massive accretion disk? *Astron. Astrophys.* **398**, 517 (2003).
 - [8] J.-M. Huré and F. Hersant, The Newtonian potential of thin disks, *Astron. Astrophys.* **531**, A36 (2011).
 - [9] J.-M. Huré, F. Hersant, C. Surville, N. Nakai, and T. Jacq, AGN disks and black holes on the weighting scales, *Astron. Astrophys.* **530**, A145 (2011).
 - [10] I. Hachisu and Y. Eriguchi, Equilibrium structures of rotating isothermal gas clouds. I, *Astron. Astrophys.* **143**, 355 (1985).

- [11] I. Hachisu, A versatile method for obtaining structures of rapidly rotating stars, *Astrophys. J. Suppl. Ser.* **61**, 479 (1986).
- [12] M. Ansorg and D. Petroff, Black holes surrounded by uniformly rotating rings, *Phys. Rev. D* **72**, 024019 (2005).
- [13] M. Shibata, Rotating black hole surrounded by self-gravitating torus in the puncture framework, *Phys. Rev. D* **76**, 064035 (2007).
- [14] J. Karkowski, P. Mach, E. Malec, M. Piróg, and N. Xie, Rotating systems, universal features in dragging and ant dragging effects, and bounds of angular momentum, *Phys. Rev. D* **94**, 124041 (2016).
- [15] J. F. G. Auchmuty and R. Beals, Variational Solutions of Some Nonlinear Free Boundary Problems, *Arch. Ration. Mech. Anal.* **43**, 255 (1971).
- [16] U. Heilig, On the Existence of Rotating Stars in General Relativity, *Commun. Math. Phys.* **166**, 457 (1995).
- [17] U. M. Schaudt and H. Pfister, The Boundary Value Problem for the Stationary and Axisymmetric Einstein Equations is Generically Solvable, *Phys. Rev. Lett.* **77**, 3284 (1996).
- [18] U. M. Schaudt, On the Dirichlet Problem for Stationary and Axisymmetric Einstein Equations, *Comm. Math. Phys.* **190**, 509 (1998).
- [19] E. Butterworth and I. Ipser, Rapidly rotating fluid bodies in general relativity, *Astrophys. J.* **200**, L103 (1975).
- [20] J. M. Bardeen, A Variational Principle for Rotating Stars in General Relativity, *Astrophys. J.* **162**, 71 (1970).
- [21] F. Galeazzi, S. Yoshida, and Y. Eriguchi, Differentially-rotating neutron star models with a parametrized rotation profile, *Astron. Astrophys.* **541**, A156 (2012).
- [22] K. Uryu, A. Tsokaros, F. Galeazzi, H. Hotta, M. Sugimura, K. Taniguchi, and S. Yoshida, New code for equilibriums and quasiequilibrium initial data of compact objects. III. Axisymmetric and triaxial rotating stars, *Phys. Rev. D* **93**, 044056 (2016).
- [23] K. Uryu, A. Tsokaros, L. Baiotti, F. Galeazzi, K. Taniguchi, and S. Yoshida, Modeling differential rotations of compact stars in equilibriums, *Phys. Rev. D* **96**, 103011 (2017).
- [24] P. Mach and E. Malec, General-relativistic rotation laws in rotating fluid bodies, *Phys. Rev. D* **91**, 124053 (2015).
- [25] Jerzy Knopik, Patryk Mach and Edward Malec, General-relativistic rotation laws in rotating fluid bodies: constant linear velocity, *Acta Phys. Pol. B* **46**, 2451 (2015).
- [26] L. G. Fishbone and V. Moncrief, Relativistic fluid disks in orbit around Kerr black holes, *Astrophys. J.* **207**, 962 (1976).
- [27] S. R. Brandt and E. Seidel, Evolution of distorted rotating black holes. I. Methods and tests, *Phys. Rev. D* **52**, 856 (1995).
- [28] Wolfram Research, Inc., *Mathematica*, Version 11.3, Champaign, IL (2018).
- [29] S. Dain and M. E. Gabach-Clement, Geometrical inequalities bounding angular momentum and charges in General Relativity, *Living Reviews in Relativity*, **21**, 5 (2018).
- [30] M. Khuri and N. Xie, Inequalities between size, mass, angular momentum, and charge for axisymmetric bodies and the formation of trapped surfaces, *Ann. Henri Poincaré* **18**, 2815 (2017).